European Journal of Neuroscience, Vol. 23, pp. 3025–3033, 2006 doi:10.1111/j.1460-9568.2006.04809.x

Optical imaging of medullary ventral respiratory network during eupnea and gasping *In situ*

Jeffrey T. Potts[1] and Julian F. R. Paton[2]
[1]Department of Biomedical Science, College of Veterinary Medicine, Dalton Cardiovascular Research Center, University of Missouri, 134 Research Park Dr, Columbia, MO 65211
[2]Department of Physiology, Bristol Heart Institute, School of Medical Sciences, University of Bristol, Bristol, UK

Keywords: pontomedullary axis, rat, respiratory pattern, respiratory rhythm, voltage-sensitive dye

Abstract

In severe hypoxia, respiratory rhythm is shifted from an eupneic, ramp-like motor pattern to gasping characterized by a decrementing pattern of phrenic motor activity. However, it is not known whether hypoxia reconfigures the spatiotemporal organization of the central respiratory rhythm generator. Using the *in situ* arterially perfused juvenile rat preparation, we investigated whether the shift from eupnea to gasping was associated with a reconfiguration of the spatiotemporal pattern of respiratory neuronal activity in the ventral medullary respiratory network. Optical images of medullary respiratory network activity were obtained from male rats (4–6 weeks of age). Part of the medullary network was stained with a voltage-sensitive dye (di-2 ANEPEQ) centred both within, and adjacent to, the pre-Bötzinger complex (Pre-BötC). During eupnea, optical signals initially increased prior to the onset of phrenic activity and progressively intensified during the inspiratory phase peaking at the end of inspiration. During early expiration, fluorescence was also detected and slowly declined throughout this phase. In contrast, hypoxia shifted the respiratory motor pattern from eupnea to gasping and optical signals were restricted to inspiration only. Areas active during gasping showed fluorescence that was more intensive and covered a larger region of the rostral ventrolateral medulla compared to eupnea. Regions exhibiting peak inspiratory fluorescence did not coincide spatially during eupnea and gasping. Moreover, there was a recruitment of additional medullary regions during gasping that were not active during eupnea. These results provide novel evidence that the shift in respiratory motor pattern from eupnea to gasping appears to be associated with a reconfiguration of the central respiratory rhythm generator characterized by changes in its spatiotemporal organization.

Introduction

Recent advances in optical imaging techniques using voltage-sensitive dyes (VSD) have provided unprecedented information of spatiotemporal activity patterns within neuronal networks. Optical imaging has been used successfully to visualize the activity of the somatosensory cortex in the *in vivo* rat (Petersen 2003a, 2003b, 2003c; Petersen *et al*., 2004; Takashima *et al*., 2005). However, due to the limited diffusion and uptake of VSDs, as well as the inherent light-scattering properties of tissue and blood, optical imaging has been limited to superficial structures (Grinvald *et al*., 1988).

Recently, VSDs have been applied to study the mammalian medullary respiratory network (Fisher *et al*., 2005; Eugenin *et al*., 2006). A series of studies by Onimaru and colleagues (Onimaru & Homma, 2003; Onimaru *et al*., 2004; Onimaru & Homma 2005b) have visualized the spatiotemporal activity of central respiratory neurons during fictive breathing *in vitro* using high-resolution optical imaging. However, to date this approach has been restricted to *in vitro* preparations of early postnatal rats, which generate respiratory motor patterns that differ considerably from those generated by *in vivo* neonatal (Fung *et al*,. 1995; Wang *et al*., 1996) and mature rats (St John, 1990). As such, the spatiotemporal activity patterns previously reported in the neonate may differ from those in more mature preparations. Therefore, it is of importance to understand the spatiotemporal organization of respiratory activity in the fully developed brainstem.

It has been shown that the generation of respiratory activity can be altered under different behavioural states. For instance, hypoxia shifts respiratory rhythm patterns from an eupneic, ramp-like phrenic motor pattern to gasping, which is characterized by a decrementing motor pattern. Although the mechanisms underlying the shift in respiratory motor pattern remain unknown, it has been suggested that separate medullary respiratory centres may generate each motor pattern (St John, 1990; Fung *et al*., 1994). Alternatively, the different motor patterns may arise from a reconfiguration of the central respiratory activity (Lieske *et al*., 2000). Therefore, the aim of the present study was to: (i) image respiratory activity within the ventrolateral medulla of a juvenile rat with a functionally intact ponto-medullary respiratory network, which some believe is required for the generation of normal breathing (Richter & Spyer, 2001; St-John & Paton, 2004), and (ii) determine whether the shift from eupnea to hypoxic-induced gasping is accompanied by a change in the spatiotemporal activity of ventral medullary respiratory neurons. The latter mechanism would support reconfiguration of central medullary respiratory activity. To this end, we have employed an *in situ* artificially perfused rat preparation that retains the pontomedullary respiratory circuit (Paton, 1996) and permits reversible shifting from the eupneic to the gasping pattern (St-John & Paton, 2000a). The cell-free perfusate, to minimize light scattering, along with mechanical stability of the brainstem due to an absence of cardiac pulsing offered by this *in situ* approach were deemed advantageous for optical imaging.

Correspondence: Dr Jeffrey T. Potts, as above.
E-mail: pottsjt@missouri.edu

Received 7 December 2005, revised 24 February 2006, accepted 28 February 2006

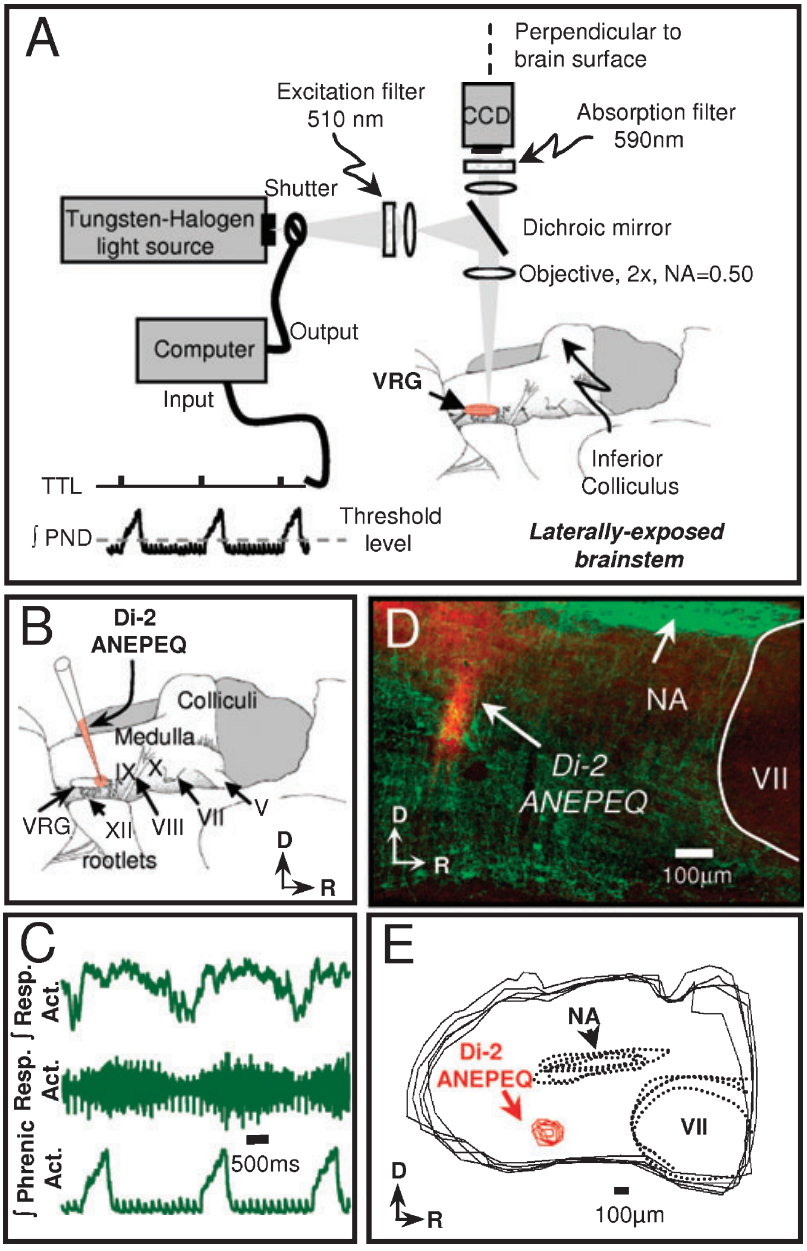

FIG. 1. (A) Schematic of experimental and optical setup for fluorescence measurements from the ventrolateral medulla. Note, the head of the preparation was rotated 90° from horizontal and the camera axis was perpendicular to the brain surface. Quenching of fluorescence was minimized by obtaining optical acquisition sweeps triggered from the onset of phrenic nerve discharge (PND). A computer generated TTL pulse opened a mechanical shutter for 1.8 s. See methods for additional details. (B) Approach used to label neurons with the voltage-sensitive dye di-2 ANEPEQ. Schematic of the exposed medulla showing cranial roots and surface of the lateral brainstem. Position of micropipette containing di-2 ANEPEQ (shaded red) is shown at the level of the rostral-most rootlet of the hypoglossal nerve. Shaded red region of the medulla represents approximate location of the ventral respiratory group (VRG) including the Pre-BötC. (C) Extracellular population activity was recorded from the micropipette prior to injection of dye to confirm location within respiratory-related regions of the VRG. (D) Immunohistochemical labelling of brainstem from one preparation illustrating location of injection site. Labelling of neurokinin$_1$ receptors (green) was used to localize respiratory populations in the ventrolateral medulla. Note, intense NK_1 immunoreactivity in the ventrolateral medulla ventral of nucleus ambiguus (NA) extending caudally from the caudal pole of the facial nucleus (VII). The location of one di-2 ANEPEQ injection site is clearly visible within the region of NK_1 immunoreactivity, which exhibited both inspiratory and expiratory activity (see B). (E) Summary of the distribution of di-2 ANEPEQ injection sites from one experiment. This figure consists of computer-assisted drawings from five sagittal sections of the medulla (alternate sections, 50-µm thick) outlining the di-2 ANEPEQ labelled region (red). V, trigeminal nerve; VIII, vestibulocochlear nerve; IX, glossopharyngeal nerve; X, vagus nerve.

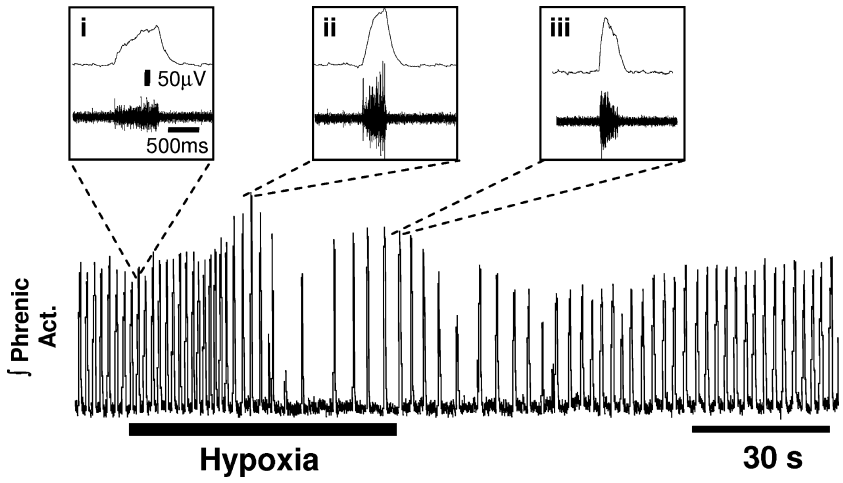

FIG. 2. Change in respiratory pattern from eupnea to gasping evoked by systemic hypoxia. The main trace is of the rectified, integrated phrenic nerve discharge prior to, during and following recovery from hypoxia. Prior to hypoxia, the preparation generated a spontaneous eupneic-like respiratory pattern of incrementing PND (see panel i). Following exposure to a hypoxic normocapnic gas mixture (10%O_2, 5% CO_2, balance N_2), respiratory frequency and amplitude initially increased (see panel ii). However, during prolonged hypoxic exposure (> 1 min), respiratory frequency declined and a decrementing pattern of PND became evident consistent with gasping (see panel iii).

Materials and methods

Experiments were performed in accordance with the National Institutes of Health guidelines for animal care and welfare. All protocols were approved in advance by the Institutional Animal Care and Use Committee at the University of Missouri.

In situ *artificially perfused rat preparation*

Experiments were performed on male Wistar rats (60–90 g, $n = 4$) using the *in situ* arterially perfused preparation (Paton, 1996). Briefly, rats were anaesthetized deeply via inhalation of halothane (5%) until they failed to show withdrawal responses to noxious pinching of the tail or a paw. Animals were bisected sub-diaphragmatically and exsanguinated. A precollicular decerebration was performed and the cerebellum removed to expose the dorsal surface of the brainstem. The left phrenic nerve was sectioned at the level of the diaphragm. The thoracic aorta was cannulated with a double lumen catheter (16 ga/18 ga, Braintree Scientific) and perfused with a Ringer solution containing an oncotic agent (Ficoll, 70 kDa, 1.25%, Sigma), gassed with 95% O_2 and 5% CO_2, warmed to 32–34 °C and filtered (polypropylene mesh, pore size 40 μm). Pump flow rate was adjusted to give a perfusion pressure of 65–85 mmHg as monitored via a pressure transducer (model P23, Statham). Neuromuscular paralysis was produced by addition of vecuronium bromide (50 μg) directly to the perfusate. Phrenic nerve discharge (PND) was recorded via a glass suction electrode and activity amplified 10 000–20 000 times (Neurolog NL104), integrated (time constant 100 ms; Neurolog NL703) and filtered (Neurolog NL126; 500 Hz–5 kHz).

Voltage-sensitive dye staining

The hydrophilic dye di-2 ANEPEQ (50 μg/mL, Molecular Probes, Eugene, OR) was microinjected directly into the ventral respiratory network from a glass micropipette (10–15 μm o.d.) via a lateral approach (see Dutschmann & Paton, 2003; Fig. 1A). Briefly, with the head rotated 90° from horizontal, a portion of the skull (including the bulla region) was removed to permit direct visualization of the cranial nerves (see Fig. 1B). Pipettes were orientated perpendicular to the medullary surface with reference to the rostral-most hypoglossal root and advanced into the medulla using a stepper motor (Inchworm, Burleigh). Population activity was recorded through this pipette and subsequently injections were made from this pipette into regions exhibiting respiratory-related discharge (Fig. 1B and C). Typically, microinjections were made at three distinct rostral-caudal sites that all displayed population respiratory activity. At each site, 50–60 nL of di-2 ANEPEQ was microinjected over a 30–45-s period. The first microinjection occurred at the level of the rostral-most hypoglossal root followed by an injection 300 μm rostral and 300 μm caudal to it. All injection sites were 800–1000 μm below the ventrolateral medullary surface. Following microinjections of di-2 ANEPEQ,

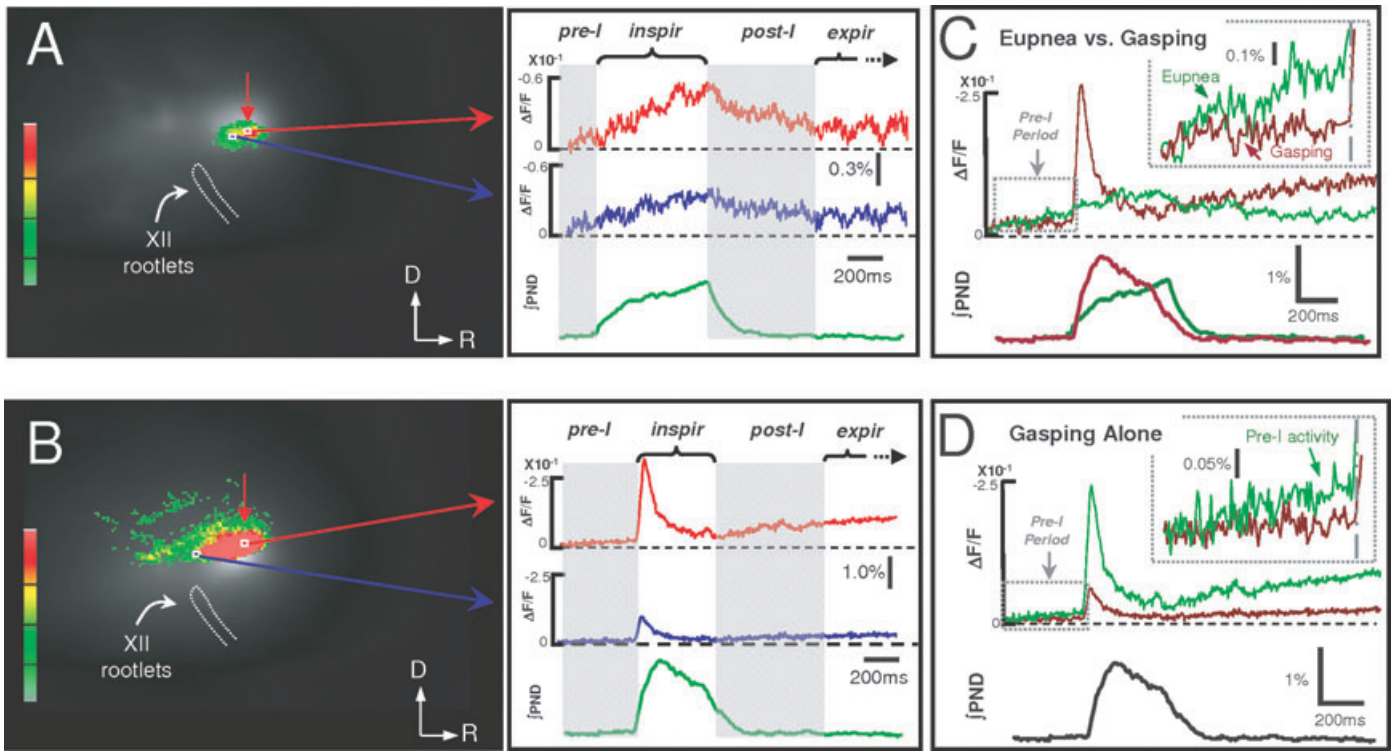

FIG. 3. Temporal pattern of optical activity in the rostral ventrolateral medulla and Pre-BötC during eupnea and gasping obtained from the same preparation. (A and B) Change in fluorescence from two regions of the medulla (red and blue squares) during eupnea (A) and gasping (B). Left panels show image of lateral brainstem with superimposed optical signals acquired at peak fluorescence in inspiration during eupnea and gasping. Scale bars represent relative per cent change in fluorescence ($\Delta F/F$ percentage) with red representing maximal fluorescence. Right panels show temporal changes in fluorescence averaged from ten phrenic nerve-triggered respiratory cycles in eupnea and from two phrenic nerve-triggered cycles in gasping. Note presence of post-inspiratory activity in eupnea but not gasping. Red arrows in A and B represent imaged regions analysed in C. (C) Temporal changes in optical activity during the pre-inspiratory period in eupnea and gasping. Fluorescent activity was greater prior to phrenic onset in eupnea compared to gasping (see inset). (D) Temporal changes in optical activity during the pre-inspiratory period from two distinct brainstem regions during gasping (see white boxes in panel B). We found that only regions of high fluorescence generated optical signals prior to phrenic onset. Note, red and blue traces in panel D are the same traces as in B. I, inspiratory phase; Pre-I, pre-inspiratory activity; ∫PND, integrated phrenic nerve discharge; XII, hypoglossal nerve rootlets. The vertical scales in A and B show $\Delta F/F$.

in situ preparations continued to exhibit eupneic-like breathing rhythms. In all preparations, basal respiratory frequency did not change by more than ± 5% following 15–30 min of dye injection and the discharge pattern of the phrenic nerve maintained its ramping eupneic-like appearance. Together, these findings indicate that the effect of dye-staining was not detrimental to central respiratory rhythm and pattern generation.

Optical imaging

The imaging field was focused on the ventrolateral surface of the medulla with the camera axis perpendicular to the brain surface (Fig. 1A). Neuronal activity was visualized as a change in fluorescence of the VSD as recorded using an optical imaging recording system (MiCAM02, Brain Vision Inc., Tsukuba, Japan). The VSD was excited using a 150 W tungsten-halogen lamp (HL-150) that was collimated, passed through a 510 nm excitation filter, a dichroic mirror and a 590 nm long-pass absorption filter. A CCD camera (8.4 mm × 6.6 mm) with high dynamic range (> 66 db), high quantal efficiency (75% @550 nm, 55% @700 nm) and maximum time resolution of 3.5 ms per frame detected the changes in fluorescence. Magnification was provided by a 2× objective (NA 0.5, Olympus Optical) resulting in an imaging area of 4.2 mm × 3.25 mm.

Acquisition of all optical signals was triggered from the onset of rectified and integrated phrenic nerve discharge using an online script file (Spike2, CED, Cambridge, UK). The script generated a TTL pulse at the onset of the phrenic nerve burst, which was used to trigger the opening of a mechanical shutter in the tungsten-halogen light source (refer to Fig. 1A). Each TTL-triggered sweep was 1.8 s in length. Typically, images were obtained at a frame rate of 3.7 ms per frame and were averaged over ten sweeps. Based on preliminary experiments, optical imaging of eupnea typically required ten acquisition sweeps, while optical imaging of gasping required only a single acquisition sweep. This was likely due to the large amplitude of fluorescence activity evoked by gasping (i.e. typically 3–5-fold greater then eupnea). However, it should be noted that when an image was obtained by averaging a greater number of phrenic cycles (i.e. 50 cycles), the relative amplitude of the optical signal and its spatiotemporal activity pattern was similar to that obtained using ten sweeps.

Several analyses were performed on the acquired optical images. First, the resulting differential image was processed using a two dimensional spatial filter (3 × 3 pixel) and pseudo-coloured such that red corresponded to maximal membrane depolarization. Second, movement artifact, or signal drift due to mechanical vibration, was removed using smoothing algorithms developed by BrainVision and finally, pixel intensities that were < 10% of the full-scale change in fluorescence were removed by thresholding to minimize background fluorescence.

Peak fluorescence was quantified by averaging pixel values of a 10 × 10 pixel square positioned over the region of maximal fluorescence. Pixel values below threshold were not included in this calculation.

Generation of hypoxic-induced gasping

The shift from a eupneic-like respiratory motor pattern to gasping was produced by changing from the perfusate reservoir aerated with carbogen (95% O_2, 5% CO_2) to one gassed with a hypoxic mixture (10% O_2, 5% CO_2, balance N_2). Gasping was defined as lower frequency (relative to eupnea) decrementing discharges of phrenic nerve activity that followed after a biphasic response of excitation and depression. Carbogen gassed perfusate was switched back after 45–55 s. At least 15 min elapsed between repeated exposures to hypoxia. Typically, we were able to shift from eupnea to gasping reversibly 4–6 times per experiment.

Immunocytochemical detection of neurokinin$_1$ (NK_1) receptors

Following each experiment, the brain was removed and fixed in 4% paraformaldehyde in 0.1 M phosphate buffer at 4 °C for 24–48 h. This was followed by cryoprotection using 30% sucrose for 12–18 h at 4 °C or until the brain sank. The brain was then trimmed to retain the medulla (including the VRG), blocked in OCT and sagittal sections of the brainstem (50-μm thick) were cut using a freezing microtome (MicroM, mode D6900). Sections were washed (4 × 10 min) in PBS (pH 7.4) at room temperature and blocked with 5% normal donkey serum (Jackson ImmunoResearch) in 0.3% Triton X in PBS. Sections were then incubated with rabbit polyclonal anti-NK_1 (1 : 1000, Novus Biologicals) overnight on a shaker at room temperature. After washing (4 × 10 min) with PBS, sections were incubated for 2 h in anti-rabbit NK_1 secondary antibody conjugated with Oregon Green (1 : 3000, Jackson ImmunoResearch). Finally, sections were washed (3 × 10 min) in PBS, transferred onto plus-coated slides and coverslipped with Vectashield (Vector Laboratories).

Histological reconstruction and imaging

A set of 50-μm-thick sagittal sections was examined using an Olympus BX-51 microscope equipped with epifluorescence and appropriate excitation/emission filter set (excitation −545 nm; emission −610 nm; dichrotic −570 nm). Images were captured using a cooled monochrome CCD camera (OCRA ER, Hamamotsu) and analysed using commercially available software (Neurolucida, MicroBrightfield). Computer-assisted drawings of the injection sites were made with a motor-driven stage and Neurolucida files were analysed using NeuroExplorer software (MicroBrightfield).

Data and statistical analyses

Values are given as mean ± SEM. Significant differences ($P < 0.05$) was determined using Student's *t*-test for paired samples.

Results

Functional localization and Pre-BötC verification of recording sites

The approach and location of dye injections was functionally confirmed online by extracellular recordings (population activity; Fig. 1C), as well as *posthoc* with immunocytochemical analysis (Fig. 1D). Each injection site in all preparations was chosen at which either inspiratory, early expiratory (post-inspiratory) or both inspiratory and early expiratory activity was recorded. Furthermore, our immunocytochemical analysis indicated that injections were located in regions of the respiratory column that contained significant NK_1 receptor immunoreactivity (Fig. 1D), which has been used as a marker for the pre-Bötzinger region (St-John & Paton, 2000b; Gray *et al*., 2001; Guyenet *et al*., 2002; Stornetta *et al*., 2003). An example of the topographical distribution of di-2

TABLE 1. Characteristics of the respiratory motor pattern during eupnea and gasping

	Eupnea	Gasping	*F*-value	*P*-value
Ti (ms)	703 ± 25	371 ± 22	100.24	0.0001
Te (ms)	1376 ± 163	2320 ± 192	14.01	0.0096
Ttot (ms)	2079 ± 186	2690 ± 207	4.84	0.0702
Freq (Hz)	0.49 ± 0.08	0.38 ± 0.03	5.01	0.0664

$n = 4$; Mean ± SEM. Statistical comparisons between eupnea vs. gasping. Ti, inspiratory time; Te, expiratory time; Ttot, respiratory duration; Freq, respiratory frequency.

ANEPEQ staining in the medulla from one experiment is shown in Fig. 1E. Computer-assisted reconstruction of sagittal brainstem sections indicated that injections were located caudal to the facial nucleus (400–500 μm) and ventral to the nucleus ambiguus (NA) 200–400 μm. Injection sites therefore encompassed both the pre-Bötzinger and rostral VRG regions.

Switching from the eupneic to gasping pattern

The respiratory response to hypoxia is shown in Fig. 2. Following exposure to hypoxia there was an initial excitation of the respiratory network shown by an increase in PND frequency and amplitude (see Fig. 2, i and ii), a period of respiratory depression and then a characteristic decrementing phrenic discharge pattern (see Fig. 2, iii). It was associated with a significant decrease in inspiratory time (Ti), an increase in expiratory time (Te), and a reduction in frequency. Similar changes in the respiratory pattern were observed when switching from eupnea to gasping in all four preparations (see Table 1). This time course and pattern of response was identical to gasping that has been described previously in this preparation (St-John & Paton, 2000a).

Temporal activity patterns of optical responses from the medullary respiratory network during eupnea and gasping

A representative example of the temporal activity patterns of optical responses recorded from regions of the medulla during eupnea and gasping is shown in Fig. 3. We imaged two areas of the medulla – a region of high and low optical activity. Both areas showed the same qualitative response pattern. During eupnea, temporal changes in fluorescence were found during late expiratory or pre-inspiratory, inspiratory and post-inspiratory (e.g. early expiratory) phases of the respiratory cycle (Fig. 3A). Thus, the temporal patterns in optical activity were first detected immediately prior to the onset of phrenic discharge. Optical signals intensified progressively in amplitude during neural inspiration reaching a peak coincident with the end of the inspiratory phase. At the beginning of expiration, fluorescence remained elevated coincident with the post-inspiratory phase and then decremented throughout the interphrenic discharge interval. These temporal activity patterns were observed in all preparations studied.

In contrast, the temporal pattern of optical activity during gasping was characterized by a very rapid onset that appeared to coincide with the onset of phrenic activity (Fig. 3B). Fluorescence activity then decayed rapidly throughout inspiration. Unlike eupnea, optical signals were virtually absent immediately following inspiration but increased monotonically throughout expiration. A comparison of the optical activity patterns during eupnea and gasping prior to the onset of phrenic discharge is shown in Fig. 3C. As these regions were spatially distinct (see arrowhead in Fig. 3A and B), this meant that we were imaging from different areas of the medulla. From the regions displaying peak optical activity during inspiration, we found that fluorescence increased to a greater extent during eupnea in the pre-inspiratory period compared to gasping (see inset Fig. 3C). However, during gasping (Fig. 3D) it was possible to find medullary regions (not active during eupnea) that also exhibited fluorescence in the pre-inspiratory phase (see inset Fig. 3D). The magnitude of pre-inspiratory optical activity during gasping was significantly less then during eupnea (0.051 ± 0.007 vs. 0.232 ± 0.055%, $n = 4$, $P < 0.05$, gasping vs. eupnea).

Spatial activity patterns of optical responses from the medullary respiratory network during eupnea and gasping

The spatial patterns of optical activity during eupnea and gasping appeared to be distinct. During eupnea (Fig. 4A, i–v), respiratory-related optical activity appeared throughout the respiratory cycle in regions receiving dye injection, which corresponded to the rostral ventral respiratory group/pre-Bötzinger complex (Pre-BötC) as defined by its position relative to the rostral-most hypoglossal root and subsequently confirmed histologically (see Fig. 1B and D). The activity rapidly propagated in the dorso-ventral and rostro-caudal directions throughout inspiration and slowly retracted during expiration. In contrast, during gasping (Fig. 4B, i–v) the level of optical activity prior to phrenic onset was significantly reduced (0.051 ± 0.007 vs. 0.232 ± 0.055%, $n = 4$, $P < 0.05$, gasping vs. eupnea) and peak fluorescence activity occurred at a much earlier phase of the inspiratory burst (35 ± 10 vs. 497 ± 67 ms, gasping vs. eupnea, $n = 4$, $P < 0.05$). Following onset of the inspiratory gasp, optical activity rapidly retracted and almost fully decayed back to baseline level at the end of inspiration. Medullary regions emitting fluorescence during gasping extended more caudally and dorsally with respect to eupnea, and the area occupied by peak fluorescence tended to be larger. The centre core of fluorescent activity during gasping shifted dorsally and the spatial boundaries extended dorso-caudally to include areas just caudal to the rostral-most rootlet of the hypoglossal nerve.

The peak level of optical activity during inspiration also differed significantly (Fig. 4C). During gasping, peak inspiratory fluorescence was approximately 270% greater then the peak level generated during eupnea, although during early expiration fluorescence levels remained relatively low during gasping compared to those measured at the same time of the respiratory cycle during eupnea (0.106 ± 0.064 vs. 0.370 ± 0.052%, $n = 4$, $P < 0.05$, gasping vs. eupnea).

To compare the spatial relationship between eupnea and gasping, regions of peak inspiratory optical activity obtained from the same experiment were superimposed (Fig. 5A). Distinct regions of intense inspiratory fluorescence overlapped minimally. In fact, the core of peak inspiratory fluorescence during gasping shifted caudally and dorsally with respect to the core of peak fluorescence during eupnea. This shift in spatial activity was observed in all preparations. To track changes in spatiotemporal activity over the respiratory cycle (i.e. 1.11 s of the 1.8 s acquisition sweep), a series of pixel images was obtained along a narrowly confined region of the medulla extending caudally from a point rostral of the hypoglossal rootlets (indicated by the solid lines in Fig. 5A). During eupnea (Fig. 5, Bi, upper panel), optical signals appeared to be restricted to a compact rostro-caudal region of the medulla. In contrast, fluorescence activity during gasping extended into a region caudal of the rostral-most hypoglossal rootlet (indicated by horizontal dashed lines in Fig. 5, Bi, lower panel). A second example illustrating a similar shift in the spatiotemporal pattern

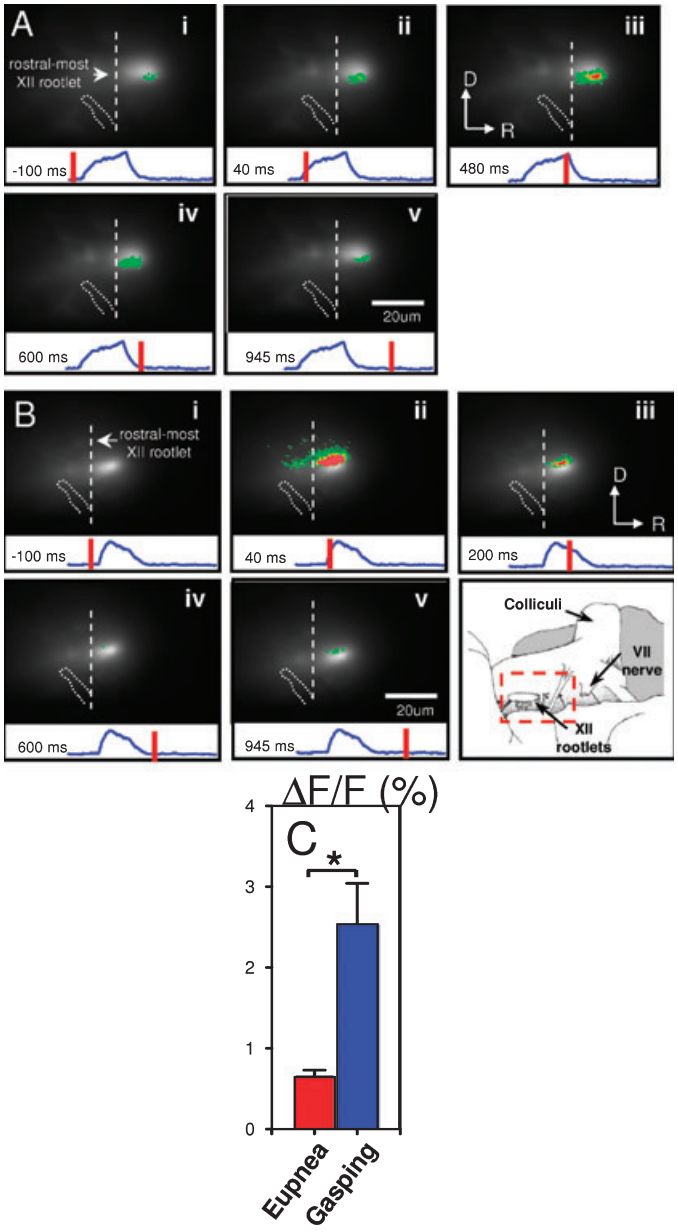

FIG. 4. Spatial activity maps of optical activity during eupnea and gasping. (A) During eupnea, fluorescence activity was present prior to phrenic onset and spread in the rostrocaudal and dorsoventral planes reaching maximal spread at the end of inspiration. Fluorescence then retracted gradually during expiration. The blue trace under each panel represents rectified and integrated phrenic nerve activity, while the red bar and numerical value represents the time at which the image was obtained relative to the respiratory cycle. The vertical white dashed line represents the approximate location of the rostral-most hypoglossal rootlet. (B) During gasping, the area of fluorescence was typically larger and extended more dorsally and caudally. Unlike eupnea, the optical activity retracted rapidly throughout inspiration and reached a nadir in early expiration. The schematic diagram shows that the area of the brainstem imaged that was the same for eupnea and gasping.(C) Average peak fluorescence evoked in inspiration during eupnea and gasping. *Significant difference between eupnea and gasping ($P < 0.05$). VII, facial nerve; XII, hypoglossal nerve rootlets.

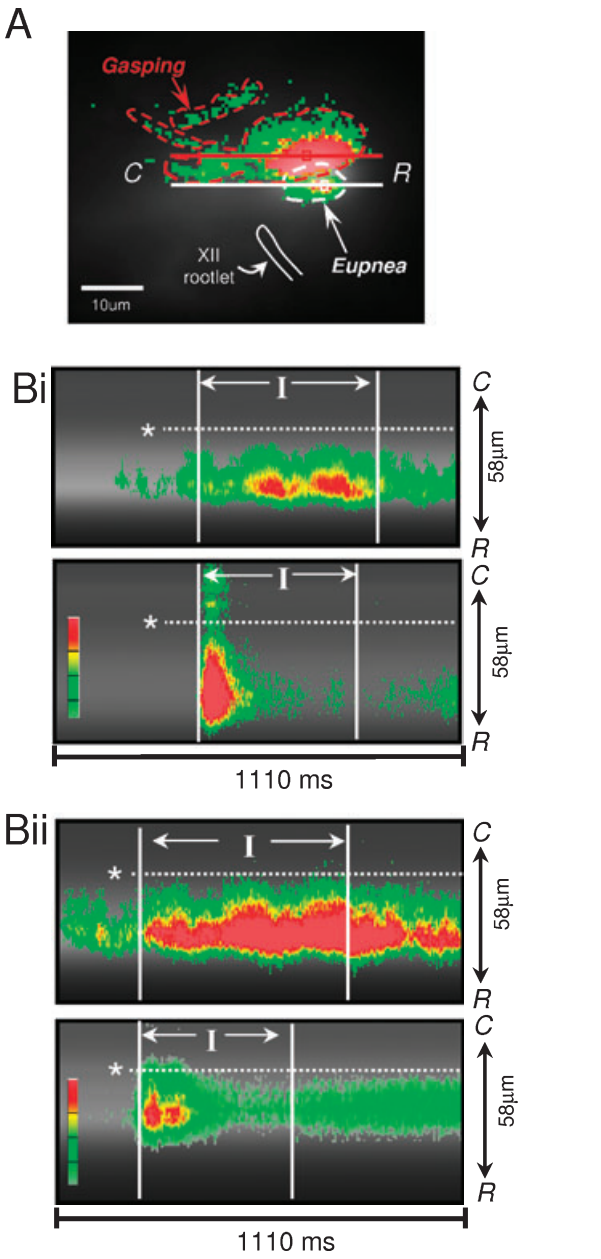

FIG. 5. (A) Maximal spread of optical activity during eupnea and gasping. The dashed lines outline the extreme spatial boundaries of optical activity in inspiration during eupnea (white dashed line) and gasping (red dashed line). The spatial activity maps overlapped minimally. (B) Spatiotemporal map of optical activity during eupnea (upper panel) and gasping (lower panel) obtained from two separate preparations (Bi and Bii). Vertical white lines represent inspiratory (I) phase. During eupnea, regions of optical activity were present throughout the respiratory cycle (i.e. pre-inspiration, inspiration, expiration). In contrast, the majority of the fluorescence during gasping occurred early in inspiration and decayed rapidly. In addition, regions of fluorescence extended more caudally and dorsally during gasping. Note, C and R represent 'caudal' and 'rostral' directions, respectively. XII, hypoglossal nerve rootlets; *level of rostral-most hypoglossal rootlet.

of optical activity from a different experiment is shown in Fig. 5, Bii. In addition, there was a clear absence of optical activity prior to inspiration during gasping.

There were several key differences in the spatial activity pattern when contrasting eupnea and gasping. First, in the same region of the rostral ventrolateral medulla, optical signals were present throughout the respiratory cycle during eupnea, albeit at different levels of optical intensity. In contrast, the same medullary region during gasping was intermittently active (i.e. the region was active in early inspiration and showed very low activity during late

inspiration and early expiration). In addition, optical activity propagated dorsally and caudally to a much greater extent during gasping compared to eupnea. Together, these findings suggest that medullary regions quiescent during eupnea may have been recruited during gasping, or alternatively, that optical signals using our imaging system may have been undetectable in these regions during eupnea.

Discussion

In the present study, we incorporated the voltage-sensitive dye, di-2 ANEPEQ, and fast optical imaging to examine changes in the spatiotemporal activity of the respiratory network in the rostral ventral respiratory group and the Pre-BötC during eupnea and hypoxic-induced gasping. We found that relative to eupnea, gasping was associated with changes in both the temporal and spatial patterns of optical activity. In particular, optical activity obtained from a small, confined region of the medulla (presumably containing the Pre-BötC) occurred throughout inspiratory and expiratory cycles during eupnea, whereas the activity during gasping occurred predominately during early inspiration. This confirms previous electrophysiological studies reporting that this region contains a heterogeneous mixture of inspiratory, expiratory and phase-spanning neurons (Rekling & Feldman, 1998; Smith *et al*., 2000). We also found that the medullary regions displaying peak fluorescence were distinct with minimal overlap during eupnea and gasping (see Fig. 5A). Similar findings have been reported in the adult cat and rat (Fung *et al*., 1994; Ramirez *et al*., 1998). It should be noted that although some optically activity regions did overlap, these areas comprised only a very small portion (∼15%) of the total active area. Together, these findings indicate that the medullary respiratory network can be reconfigured temporally and spatially under extreme states. Our data also suggest that distinct regions of the rostral ventrolateral medulla may be recruited during gasping.

The present study is the first to optically image medullary respiratory activity during eupnea and gasping in a mature mammal. It demonstrates the feasibility of the approach which until now has been restricted to reduced preparations of the neonatal rat (Onimaru *et al*., 1995; Onimaru *et al*., 1996; Onimaru & Homma, 2003; Onimaru & Homma, 2005b). We wish to point out a number of limitations with the present study that should be borne in mind. First, dye loading was limited due to the number of injections and the spread of dye from these sites. In preliminary experiments, we varied the dye concentration (5, 50, 100 μg/mL) and found that optimal images were obtained when dye concentration was 50 μg/mL. At dye concentration of 100 μg/mL, central respiratory and phrenic activities declined rapidly suggesting that this dose was toxic to respiratory neurons. In contrast, central respiratory and phrenic activities persisted for several hours following dye injections using 50 μg/mL. It was inevitable that this technique of dye delivery would not encompass the entire respiratory network. Nevertheless, we found that the injected dye reached parts of the respiratory network coinciding with the rostral ventral respiratory group and Pre-BötC. Second, dye loading via injection was uneven with higher concentrations centred at the site of each injection. This will bias optical measurements some what. It should be possible in the future to load the dye by diffusion after restrictive topical application. Indeed, removal of the lateral edge of the ventrolateral medulla as described previously (Dutschmann & Paton, 2003) may also assist dye penetration into the respiratory network. Finally, a problem inherent with the optical imaging technique concerns the depth over which we were sampling. We cannot be completely confident as to the volume of tissue we were sampling from. However, we are confident that we sampled from regions rich in respiratory neurons based on the population activity recorded prior to each dye injection (see Fig. 1C) and the subsequent respiratory-related nature of the optical signals recorded.

We employed the *in situ* model as this preparation is capable of generating a respiratory motor activity that, albeit at a slower overall frequency, is similar to the pattern generated by *in vivo* models (St-John & Paton, 2000b). During eupnea, we reported that respiratory-related changes in fluorescence occurred within a confined region of the ventrolateral medulla throughout inspiration and expiration. This area was localized well within the area loaded with dye (see Fig. 1D). Based on our anatomical reconstruction of the dye injection sites, the imaged regions were typically located 300–400 μm caudal of the facial nucleus and ventral to the compact formation of the nucleus ambiguus. The region of dye labelling extended in the rostrocaudal plane 200–300 μm and in the mediolateral plane 250–300 μm. Thus, the majority of the recorded optical activity appeared to reside in a portion of the VRG that corresponded to its rostral extent and the Pre-BötC region (Stornetta *et al*., 2003). It has been suggested that the Pre-BötC *in vitro* predominately contains inspiratory neurons, some of which possess pacermaker-like properties (Feldman *et al*., 1990; Smith *et al*., 1991). However, *in vivo* it has been shown that the Pre-BötC is composed of a heterogeneous population of respiratory neurons that also contain inspiratory cells that lack pacemaker-like properties (Schwarzacher *et al*., 1995) along with neurons possessing expiratory-related firing patterns (St-John & Paton, 2000b). Indeed, from the recordings we made prior to each dye injection, both inspiratory and early, decrementing expiratory related population activity was recorded routinely. Together, these data support our optical findings that imaged regions, which included the Pre-BötC, contain both inspiratory and early expiratory neurons.

An interesting finding from the present study was the relatively high level of optical activity in early expiration (presumably post-inspiration) during eupnea. This is in contrast with recent studies that have utilized similar optical imaging techniques to record central respiratory activity in the neonate rat *in vitro* (Onimaru & Homma, 2003; Onimaru & Homma, 2005a). In these studies, optical activity was found in spatially similar regions of the ventrolateral medulla. However, the temporal pattern of activity was restricted to inspiration. This difference is unlikely to be related to developmental changes of the respiratory network between neonate and juvenile rats, as we have previously recorded post-inspiratory activity from the ventrolateral medulla in the *in situ* neonatal rat (Dutschmann & Paton, 2003). The presence of post-inspiratory activity may reflect a functional pontine respiratory circuit in the *in situ* arterially perfused preparation that contributes to the generation of respiratory patterns and rhythms in this model that is absent in the *in vitro* slice or medullary *en bloc* preparation; this remains controversial and needs to be validated.

During gasping, we found that phasic increases in fluorescence occurred only during inspiration suggesting that the respiratory network shifted to a predominantly inspiratory-driven motor pattern with a loss of post-inspiratory activity. These findings are in agreement with previous studies that reported the onset of gasping was associated with a generalized depression of expiratory neuronal activity (Remmers *et al*., 1986; Richter *et al*., 1987; St John *et al*., 1989; Richter *et al*., 1991; Thuot *et al*., 2001). We also reported that the amplitude of peak fluorescence was 2.5 times greater during gasping than eupnea. This could be explained by: (i) increased depolarization rate and level of active inspiratory neurons; (ii) recruitment of neurons which were normally quiescent during eupnea and/or (iii) recruitment of expiratory neurons to depolarize during

inspiration. Evidence for the latter mechanism has been reported previously (Busselberg *et al*., 2001; Markstahler *et al*., 2002; Dutschmann & Paton, 2002). It has also been shown that post-inspiratory activity is lost during hypoxic-induced gasping (Dutschmann & Paton, 2005) and that post-inspiratory neurons shift their phase of activation to coincidence with inspiration (Paton *et al*., 2006). These previous results, in conjunction with the present data, support the notion that a shift from eupnea to gasping results in a reconfiguration of the respiratory network (i.e. from an inspiratory-post-inspiratory-expiratory driven pattern to an exclusively inspiratory driven pattern) that is dependent, in part, on a hypoxic-induced reduction of synaptic inhibition within the respiratory network.

We found that during hypoxic exposure there was a slow, progressive increase in optical activity reflecting membrane depolarization throughout the respiratory cycle, which was not observed during eupnea (compare Fig. 3A and B). This deserves a brief comment. Currently, we can only speculate on the cause(s) for this change in baseline fluorescence. Prolonged hypoxic exposure is likely to affect membrane conductance causing neuronal depolarization, perhaps by inactivation of an outward potassium current (Girard & Lesage, 2004), or by the failure of inhibitory processes intrinsic to the respiratory network such as GABAergic and glycinergic inhibition (Richter & Spyer, 2001; Gao *et al*., 2004; Paton & St-John, 2005a, 2005b). Both of these mechanisms are essential in coordinating respiratory motor outputs to cranial and spinal targets (Richter & Spyer, 2001). We propose that any combination of these mechanisms could account for this drift in basal fluorescence during hypoxia.

We found that the magnitude of pre-inspiratory activity was also curtailed during hypoxia and consistent with a recent study (Paton *et al*., 2006). This is suggestive of a tighter synchronization of the neuronal elements involved in mediating the burst discharge of gasping. Indeed, these optical signals are consistent with cellular data demonstrating that pre-inspiratory firing recorded from pre-inspiratory neurons was of greater duration during eupnea than during hypoxic-induced gasping (St-John & Paton, 2003). We submit that in the present study, some of the pre-inspiratory (or late expiratory) optical activity may also have originated from tonic and augmenting expiratory neurons. However, we feel that this was likely limited by the paucity of augmenting expiratory neurons in this region of the medulla.

In the present study, we also found that regions of peak fluorescence during inspiration were distinct and non-overlapping in eupnea and gasping. During gasping, inspiratory optical signals shifted caudally and dorsally relative to activated inspiratory regions during eupnea. This spatial shift is consistent with the location of chemical lesions that have been shown to abolish gasping but spared eupnea in *in vivo* rats (Fung *et al*., 1994; Huang *et al*., 1997) and cats (Ramirez *et al*., 1998). This finding may indicate the recruitment of additional neurons during gasping. However, we cannot rule out that this region may have also been active during eupnea but its activity was below the sensitivity level of our imaging system to detect changes in fluorescence. Nevertheless, this provocative finding waits future testing as to whether different neuronal pools are employed for gasping.

In conclusion, our study has shown that voltage sensitive dyes can be used to visualize optical respiratory activity from the rostral ventral respiratory group and Pre-BötC in the ponto-medullary intact *in situ* juvenile rat. The shift in respiratory pattern from eupnea to gasping is associated with a dramatic alteration in the spatiotemporal pattern of fluorescence suggesting a profound reconfiguration of neuronal activity within the central medullary respiratory network. Thus, voltage sensitive dyes together with high-speed optical imaging can be used to provide information on the spatiotemporal dynamics of the mammalian respiratory network *in situ* during changes in behavioural state.

Acknowledgements

We would like to extend our sincere thanks to Brain Vision, Inc. and SciMedia Inc. for the opportunity to use the MiCAM2 optical recording system and for their excellent technical assistance, guidance and support during this work. The study was supported by NIH grant HL059167 (JTP).

Abbreviations

NK_1, neurokinin$_1$; Pre-BötC, pre-Bötzinger complex; VSD, voltage-sensitive dyes.

References

Busselberg, D., Bischoff, A.M., Becker, K., Becker, C.M. & Richter, D.W. (2001) The respiratory rhythm in mutant oscillator mice. *Neurosci. Lett.*, **316**, 99–102.

Dutschmann, M. & Paton, J.F. (2002) Glycinergic inhibition is essential for co-ordinating cranial and spinal respiratory motor outputs in the neonatal rat. *J. Physiol.*, **543**, 643–653.

Dutschmann, M. & Paton, J.F. (2003) Whole cell recordings from respiratory neurones in an arterially perfused *in situ* neonatal rat preparation. *Exp. Physiol.*, **88**, 725–732.

Dutschmann, M. & Paton, J.F. (2005) Dynamic changes in glottal resistance during exposure to severe hypoxia in neonatal rats *in situ*. *Pediatr. Res.*, **58**, 193–198.

Eugenin, J., Nicholls, J.G., Cohen, L.B. & Muller, K.J. (2006) Optical recording from respiratory pattern generator of fetal mouse brainstem reveals a distributed network. *Neuroscience*, **137**, 1221–1227.

Feldman, J.L., Smith, J.C., Ellenberger, H.H., Connelly, C.A., Liu, G.S., Greer, J.J., Lindsay, A.D. & Otto, M.R. (1990) Neurogenesis of respiratory rhythm and pattern: emerging concepts. *Am. J. Physiol.*, **259**, R879–R886.

Fisher, J.A., Marchenko, V.A., Yodh, A.G. & Rogers, R.F. (2005) Spatiotemporal activity patterns during respiratory rhythmogenesis in the rat ventrolateral medulla. *J. Neurophysiol.*, **95**, 1982–1991.

Fung, M.L., Tomori, Z. & St John, W.M. (1995) Medullary neuronal activities in gasping induced by pharyngeal stimulation and hypoxia. *Respir. Physiol.*, **100**, 195–202.

Fung, M.L., Wang, W. & St John, W.M. (1994) Medullary loci critical for expression of gasping in adult rats. *J. Physiol.*, **480**, 597–611.

Gao, L., Lyons, A.R. & Greenfield, L.J. Jr (2004) Hypoxia alters GABAA receptor function and subunit expression in NT2-N neurons. *Neuropharmacology*, **46**, 318–330.

Girard, C. & Lesage, F. (2004) Neuronal background two-P-domain potassium channels: molecular and functional aspects. *Med. Sci. (Paris)*, **20**, 544–549.

Gray, P.A., Janczewski, W.A., Mellen, N., McCrimmon, D.R. & Feldman, J.L. (2001) Normal breathing requires preBotzinger complex neurokinin-1 receptor-expressing neurons. *Nature Neurosci.*, **4**, 927–930.

Grinvald, A., Frostig, R.D., Lieke, E. & Hildesheim, R. (1988) Optical imaging of neuronal activity. *Physiol. Rev.*, **68**, 1285–1366.

Guyenet, P.G., Sevigny, C.P., Weston, M.C. & Stornetta, R.L. (2002) Neurokinin-1 receptor-expressing cells of the ventral respiratory group are functionally heterogeneous and predominantly glutamatergic. *J. Neurosci.*, **22**, 3806–3816.

Huang, Q., Zhou, D. & St John, W.M. (1997) Lesions of regions for *in vitro* ventilatory genesis eliminate gasping but not eupnea. *Respir. Physiol.*, **107**, 111–123.

Lieske, S.P., Thoby-Brisson, M., Telgkamp, P. & Ramirez, J.M. (2000) Reconfiguration of the neural network controlling multiple breathing patterns: eupnea, sighs and gasps. *Nature Neurosci.*, **3**, 600–607.

Markstahler, U., Kremer, E., Kimmina, S., Becker, K. & Richter, D.W. (2002) Effects of functional knock-out of alpha 1 glycine-receptors on breathing movements in oscillator mice. *Respir. Physiol. Neurobiol.*, **130**, 33–42.

Onimaru, H., Arata, A., Arata, S., Shirasawa, S. & Cleary, M.L. (2004) *In vitro* visualization of respiratory neuron activity in the newborn mouse ventral medulla. *Brain Res. Dev. Brain Res.*, **153**, 275–279.

Onimaru, H., Arata, A. & Homma, I. (1995) Intrinsic burst generation of preinspiratory neurons in the medulla of brainstem-spinal cord preparations isolated from newborn rats. *Exp. Brain Res.*, **106**, 57–68.

Onimaru, H. & Homma, I. (2003) A novel functional neuron group for respiratory rhythm generation in the ventral medulla. *J. Neurosci.*, **23**, 1478–1486.

Onimaru, H. & Homma, I. (2005a) Developmental changes in the spatio-temporal pattern of respiratory neuron activity in the medulla of late fetal rat. *Neuroscience*, **131**, 969–977.

Onimaru, H. & Homma, I. (2005b) Optical imaging of respiratory neuron activity from the dorsal view of the lower brainstem. *Clin. Exp. Pharmacol. Physiol.*, **32**, 297–301.

Onimaru, H., Kanamaru, A. & Homma, I. (1996) Optical imaging of respiratory burst activity in newborn rat medullary block preparations. *Neurosci. Res.*, **25**, 183–190.

Paton, J.F. (1996) A working heart-brainstem preparation of the mouse. *J. Neurosci. Meth.*, **65**, 63–68.

Paton, J.F., Abdala, A.P., Koizumi, H., Smith, J.C. & St-John, W.M. (2006) Respiratory rhythm generation during gasping depends on persistent sodium current. *Nature Neurosci.*, **9**, 311–313.

Paton, J.F. & St-John, W.M. (2005a) Long-term intracellular recordings of respiratory neuronal activities *in situ* during eupnea, gasping and blockade of synaptic transmission. *J. Neurosci. Meth.*, **147**, 138–145.

Paton, J.F. & St-John, W.M. (2005b) Long-term intracellular recordings of respiratory neuronal activities *in situ* during eupnea, gasping and blockade of synaptic transmission. *J. Neurosci. Meth.*, **147**, 138–145.

Petersen, C.C. (2003a) The barrel cortex – integrating molecular, cellular and systems physiology. *Pflugers Arch.*, **447**, 126–134.

Petersen, C.C., Brecht, M., Hahn, T.T. & Sakmann, B. (2004) Synaptic changes in layer 2/3 underlying map plasticity of developing barrel cortex. *Science*, **304**, 739–742.

Petersen, C.C., Grinvald, A. & Sakmann, B. (2003b) Spatiotemporal dynamics of sensory responses in layer 2/3 of rat barrel cortex measured *in vivo* by voltage-sensitive dye imaging combined with whole-cell voltage recordings and neuron reconstructions. *J. Neurosci.*, **23**, 1298–1309.

Petersen, C.C., Hahn, T.T., Mehta, M., Grinvald, A. & Sakmann, B. (2003c) Interaction of sensory responses with spontaneous depolarization in layer 2/3 barrel cortex. *Proc. Natl Acad. Sci. USA*, **100**, 13638–13643.

Ramirez, J.M., Schwarzacher, S.W., Pierrefiche, O., Olivera, B.M. & Richter, D.W. (1998) Selective lesioning of the cat pre-Botzinger complex *in vivo* eliminates breathing but not gasping. *J. Physiol.*, **507**, 895–907.

Rekling, J.C. & Feldman, J.L. (1998) PreBotzinger complex and pacemaker neurons: hypothesized site and kernel for respiratory rhythm generation. *Annu. Rev. Physiol.*, **60**, 385–405.

Remmers, J.E., Richter, D.W., Ballantyne, D., Bainton, C.R. & Klein, J.P. (1986) Reflex prolongation of stage I of expiration. *Pflugers Arch.*, **407**, 190–198.

Richter, D.W., Ballantyne, D. & Remmers, J.E. (1987) The differential organization of medullary post-inspiratory activities. *Pflugers Arch.*, **410**, 420–427.

Richter, D.W., Bischoff, A., Anders, K., Bellingham, M. & Windhorst, U. (1991) Response of the medullary respiratory network of the cat to hypoxia. *J. Physiol.*, **443**, 231–256.

Richter, D.W. & Spyer, K.M. (2001) Studying rhythmogenesis of breathing: comparison of *in vivo* and *in vitro* models. *TINS*, **24**, 464–472.

Schwarzacher, S.W., Smith, J.C. & Richter, D.W. (1995) Pre-Botzinger complex in the cat. *J. Neurophysiol.*, **73**, 1452–1461.

Smith, J.C., Butera, R.J., Del Koshiya, N.N.C., Wilson, C.G. & Johnson, S.M. (2000) Respiratory rhythm generation in neonatal and adult mammals: the hybrid pacemaker-network model. *Respir. Physiol.*, **122**, 131–147.

Smith, J.C., Ellenberger, H.H., Ballanyi, K., Richter, D.W. & Feldman, J.L. (1991) Pre-Botzinger complex: a brainstem region that may generate respiratory rhythm in mammals. *Science*, **254**, 726–729.

St John, W.M. (1990) Neurogenesis, control, and functional significance of gasping. *J. Appl. Physiol.*, **68**, 1305–1315.

St John, W.M., Zhou, D. & Fregosi, R.F. (1989) Expiratory neural activities in gasping. *J. Appl. Physiol.*, **66**, 223–231.

St-John, W.M. & Paton, J.F. (2000a) Characterizations of eupnea, apneusis and gasping in a perfused rat preparation. *Respir. Physiol.*, **123**, 201–213.

St-John, W.M. & Paton, J.F. (2000b) Characterizations of eupnea, apneusis and gasping in a perfused rat preparation. *Respir. Physiol.*, **123**, 201–213.

St-John, W.M. & Paton, J.F. (2003) Respiratory-modulated neuronal activities of the rostral medulla which may generate gasping. *Respir. Physiol. Neurobiol.*, **135**, 97–101.

St-John, W.M. & Paton, J.F. (2004) Role of pontile mechanisms in the neurogenesis of eupnea. *Respir. Physiol. Neurobiol.*, **143**, 321–332.

Stornetta, R.L., Rosin, D.L., Wang, H., Sevigny, C.P., Weston, M.C. & Guyenet, P.G. (2003) A group of glutamatergic interneurons expressing high levels of both neurokinin-1 receptors and somatostatin identifies the region of the pre-Botzinger complex. *J. Comp. Neurol.*, **455**, 499–512.

Takashima, I., Kajiwara, R. & Iijima, T. (2005) Voltage-sensitive dye imaging of intervibrissal fur-evoked activity in the rat somatosensory cortex. *Neurosci. Lett.*, **381**, 258–263.

Thuot, F., Lemaire, D., Dorion, D., Letourneau, P. & Praud, J.P. (2001) Active glottal closure during anoxic gasping in lambs. *Respir. Physiol.*, **128**, 205–218.

Wang, W., Fung, M.L., Darnall, R.A. & St John, W.M. (1996) Characterizations and comparisons of eupnoea and gasping in neonatal rats. *J. Physiol.*, **490**, 277–292.